Cross-linked polymers for nanofabrication of high-resolution zone plates in nickel and germanium

G. Schneider, T. Schliebe, and H. Aschoff
Georg-August-Universität Göttingen, Forschungseinrichtung Röntgenphysik, Geiststrasse 11, 37073 Göttingen, Germany

(Received 2 June 1995; accepted 16 August 1995)

A high resolution cross-linked PMMA resist has been synthesized and optimized for the generation of zone plate patterns down to 19 nm linewidth with e-beam lithography. This resist shows an increased resolution compared to PMMA for generating periodic structures with a line to space ratio of 1:1. Furthermore, we developed a cross-linked copolymer based on styrene and divinylbenzene, which is used in a new trilevel reactive ion etching (RIE) process. In this process a resist pattern of low aspect ratio can be transferred into a copolymer galvanoform with high aspect ratios for the electrodeposition of nickel. The copolymer has also been used as a highly selective etching mask for zone plate pattern transfer into germanium by RIE.

I. INTRODUCTION

Modern x-ray microscopy applications require zone plates (ZPs) with high resolution, i.e., small outermost zone width, and high efficiency. Figure 1 shows the first-order diffraction efficiency at 2.4 nm wavelength for the materials silicon, germanium, and nickel as a function of the zone thickness. These calculations are based on the coupled wave theory, which has been applied to ZPs.[1] Herein the ZP structures for the different zone width regions are approximated by a grating pattern with the corresponding local zone width. The resulting differential equations for grating structures illuminated with x rays were solved with matrix algorithms.[2] A rectangular profile of the structures is assumed in these calculations. This allows us to directly characterize the quality of the manufacturing process by comparison with experimentally derived efficiency data of ZPs. Furthermore, it follows from the theory that with Ge, and especially with Ni, high resolution and high diffraction efficiency can be combined at 2.4 nm wavelength, whereas the diffraction efficiency of Si grating structures decreases significantly from 23.8% in the 40 nm linewidth region to 14.4% in the 20 nm linewidth region.

However, it is difficult to transfer a high resolution ZP pattern generated by an e-beam lithography system in PMMA resist into Ge or Ni structures with a high aspect ratio. Our experiments showed that especially for the generation of periodic structures smaller than about 30 nm linewidth, the tolerable dose range of the e-beam exposure becomes very small, and the etch resistance of the PMMA structures during the dry etching process is degraded. In this article we describe the basic ideas and methods to improve the resist for highest resolution. Furthermore, our technology for nanofabrication of Ni and Ge ZPs is presented.

II. CROSS-LINKED PMMA ELECTRON BEAM RESIST

It was shown that an 8-nm-wide line and space pattern with a period of 100 nm can be recorded in PMMA by e-beam lithography.[3] Nevertheless, our theoretical investigations using the quantum yield for chain scission indicate that conventional PMMA—it consists of linear chain molecules—is not favorable for generating periodic structures below 30 nm linewidth and a line to space ratio of 1:1. After e-beam exposure with an electron dose of 170 μC/cm^2 using 40 keV electrons, the generated polymer chain fragments have an average length of 10–15 nm. This means that especially for periodic structures with a line to space ratio of 1:1 the difference in solubility of the exposed and unexposed lines is lowered with decreasing linewidth. The basic idea to extend the tolerable dose range and to overcome the resolution limit of PMMA for periodic structures was to cross link the linear polymer chains by adding a molecule with two reactive centers. This results in an unsoluble three-dimensional cross-linked giant molecule of infinite molecular weight where only the e-beam exposed regions dissolve in a developer after exposure. Roberts has introduced cross-linked PMMA.[4] After his work a host of other cross-linked PMMA have been reported, which are mainly developed to enhance the etch resistance of PMMA. An overview is given in Ref. 5, but to our knowledge it has not been reported that cross-linked PMMA was used to increase the resolution of PMMA for generating the smallest periodic structures.

For our purpose we polymerized the monomers methyl methacrylate (MMA) and the cross-linking molecule triethylene glycol dimethacrylate (TEGDMA) by radical reactions initiated with benzoyl peroxide. Figure 2 shows the chemical structure of this resist including the cross-linking triethylene glycol bridge, which can also be broken during e-beam exposure. The degree of cross linking is regulated by the ratio R of TEGDMA to MMA molecules. In practice 0.2 g of the radical starter is dissolved in a mixture of 6 ml MMA and 0.17 ml TEGDMA for $R = 1{:}100$. Afterwards the solution is heated to 90 °C. The radical reactions are interrupted after 5 min by cooling it down to room temperature. At this point the viscosity of the polymer is still not too high and the polymer can be dissolved in 2-methoxyethyl acetate and spin coated on a substrate. The resulting resist thickness is measured after further polymerization at 90 °C for 24 h.

The ratio R regulates the degree of cross linking, which determines the resolution and the sensitivity of the resist. R was altered to find an acceptable combination of high reso-

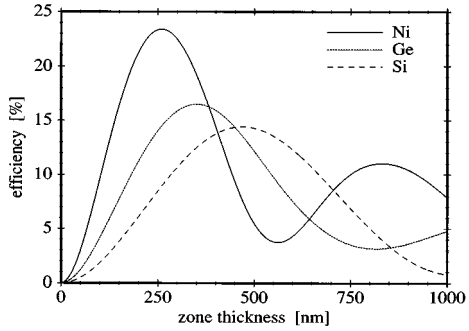

FIG. 1. First-order diffraction efficiencies at 2.4 nm wavelength of nickel, germanium, and silicon zone plates with a line to space ratio of 1:1 and rectangular zone profile as a function of the zone thickness in the 20 nm zone width regions. Other parameters: untilted zone structures and imaging magnification 1000×.

lution and a dose to be exposed in acceptable times. We performed the lithography on about 100-nm-thick silicon substrates with an Akashi DS 130-C scanning electron microscope (SEM) operating at 40 keV, which is adapted to an ELPHY III vector scan lithography device.[6–8] For $R=1{:}30$, 1:100, 1:150, and 1:300, line structures were generated with doses of $\geqslant$3000, 320, 180, and 150 μC/cm^2, respectively. In addition, the generated ZP structures recorded in cross-linked PMMA have shown no tendency to displace during the manufacturing steps, whereas under the same conditions the PMMA structures tend to displace, especially for zone widths below 30 nm. Figure 3 shows a differential interference contrast image of the ZP pattern with 20 nm outermost zone widths recorded in this resist ($R=1{:}100$) and transferred by a reactive ion etching (RIE) technique into a styrene/divinylbenzene copolymer. Note the cross resulting from the interaction of the ZP with the polarized light from the microscope, which has shown to be a reliable indication for the quality of periodic structures. The homogeneity of the cross shows that periodic resist structures down to 19 nm linewidth have been generated.

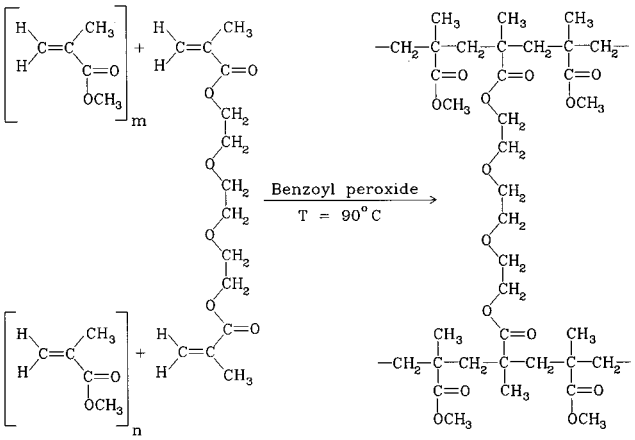

FIG. 2. Synthesis of the cross-linked PMMA by radical reactions of methylmethacrylate and triethylene glycol dimethacrylate started with benzoyl peroxide at 90 °C.

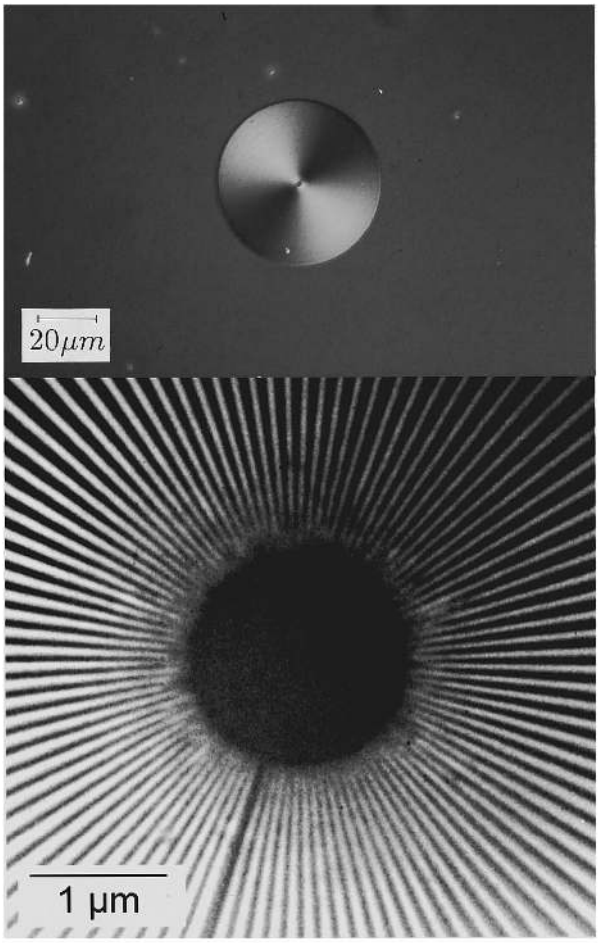

FIG. 3. Differential interference contrast (DIC) image of a copolymer ZP pattern with 20 nm smallest linewidth (top) and x-ray image of a Siemens star taken with a germanium ZP with 19 nm outermost zone width (bottom).

III. CROSS-LINKED COPOLYMER AS GALVANOFORM FOR ELECTROPLATED NICKEL ZONE PLATES

Ni structures with high aspect ratios can be generated by electroplating. It is possible to use the e-beam resist structures directly as a galvanoform for electrodeposition,[9] but it is difficult to combine small linewidths with high aspect ratios. We developed a process in which small resist lines with a low aspect ratio are transferred into a high aspect ratio galvanoform by RIE. Experiments have shown that a PMMA galvanoform is not suitable for this application, because after RIE with O_2 we observed that the electrodeposition of Ni starts on the sidewalls. We suppose that the chemical changes of PMMA during the RIE process cause a currentless deposition of Ni on the sidewalls in the electroplating bath. Therefore, a polymer with lowest electrical conductivity, high mechanical stability, and high etching rate during RIE with O_2 was developed. The galvanoform also has to have hydrophobic properties, which avoids the embedding of water and changes of the galvanoform during electroplating.

These properties were achieved with a copolymer consisting of styrene and divinylbenzene monomers with a molecule ratio of 3.1:1. In opposition to PMMA as a galvanoform, this polymer shows no sidewall growth of Ni after

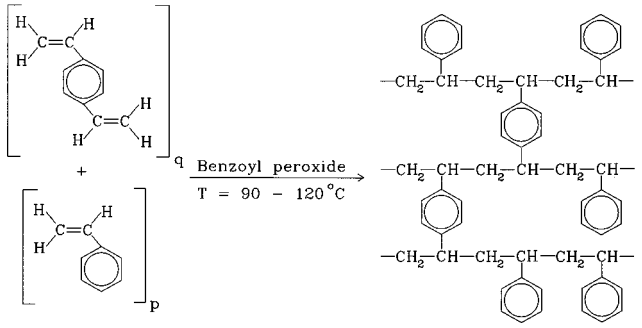

FIG. 4. Scheme for the chemical reactions of styrene and divinylbenzene initiated with benzoyl peroxide at 90 °C to achieve three-dimensional cross-linked copolymer chains.

RIE. The radical polymerization was initiated with benzoyl peroxide at a temperature of 90–100 °C; after 5 min the polymerization was stopped by cooling. Afterwards this mixture was spin coated on a substrate and highly cross linked by further radical reactions at 100–120 °C for 72 h (Fig. 4). The viscosity of the mixture and thus the resulting thickness on a substrate can be increased by starting the polymerization of the mixture again by heating it to 90 °C.

The layer sequence for the ZP generation is shown in Fig. 5. The layers are deposited by electron beam evaporation and by spin coating on 100–120-nm-thick silicon support foils. After exposure and development [Fig. 5(a)], the resist structures were transferred into a Ti layer by RIE with BCl_3 [Fig. 5(b)]. This thin layer serves as a mask for structuring the copolymer layer by RIE with O_2 [Fig. 5(c)]. This galvanoform was filled by electrodeposition in a Ni sulphamate bath operating at a temperature of 35 °C and a *p*H value of 3.5 [Fig. 5(d)]. The sequence of the Ge and Cr layers working as a plating base combines a sufficient electrical conductivity with low sputter rate during O_2–plasma etching to avoid sidewall growth during electroplating. Finally the Ti and copolymer structures are removed by RIE [Figs. 5(e) and 5(f)]. Figure 6 gives an overview of 150–170-nm-thick Ni zones and shows the uniform electrodeposition. The main advantage of our new process is that the resist thickness can be chosen independently from the required ZP thickness. Up to

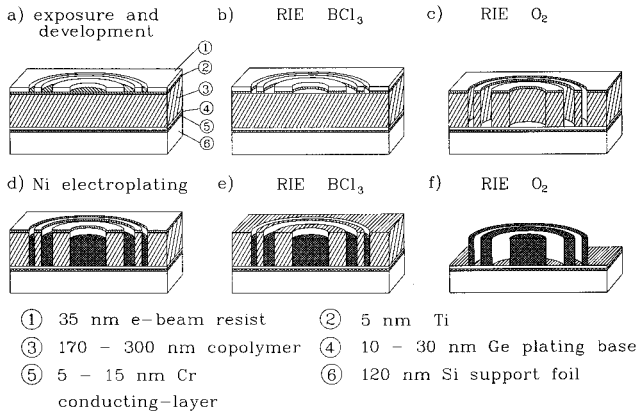

FIG. 5. Processing steps for the manufacture of electroplated nickel ZPs.

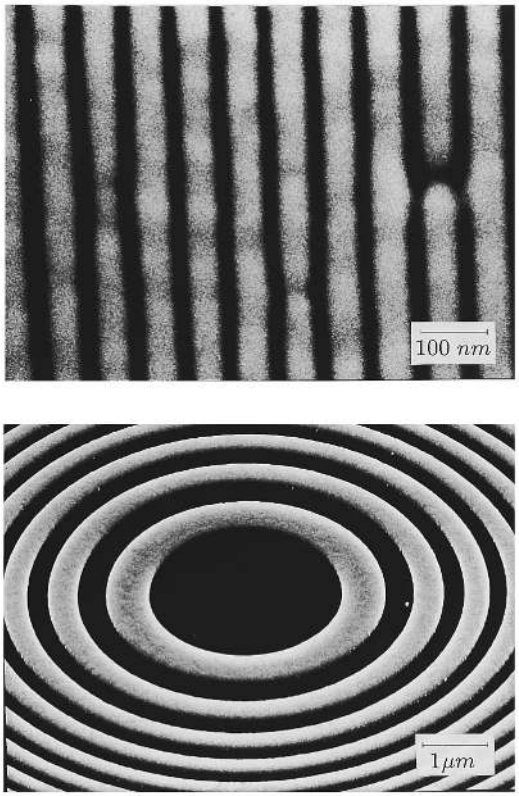

FIG. 6. SEM micrograph of the central and the outermost regions of a nickel zone plate with 170 nm height after electrodeposition and removal of the copolymer.

now aspect ratios of 6:1 have been realized by RIE techniques. It is expected that higher aspect ratios can be achieved with microwave electron cyclotron resonance discharge etching.

IV. COPOLYMER MASK FOR GERMANIUM ZONE PLATES

The RIE process for generation of high aspect ratio Ge structures requires a highly selective etching mask. We found that our copolymer, which is based on aromatic compound and is highly cross linked is more favorable as a mask compared to AZ1350 photoresist.[7,10,11] The selectivity during the Ge etching process in a $CBrF_3$–plasma is enhanced by a factor of about 1.6 compared to a AZ1350 mask. This is due to the giant molecular structure of the copolymer, which also reduces sputtering of the mask.

Figure 7 shows the processing steps for Ge ZPs. After e-beam exposure and development the resist structures were transferred in an intermediate layer of Ti by RIE with BCl_3 or Ge by RIE with $CBrF_3$ [Fig. 7(b)]. It resulted that an intermediate Ge layer causes no micromasking during the further structuring steps, whereas the resist adheres much better to a Ti layer. This adhesion becomes more important for processing structures smaller than 30 nm, because the resist structures tend to displace on the intermediate layer during the resist development. Afterwards the copolymer layer was etched with an O_2–plasma [Fig. 7(c)]. These struc-

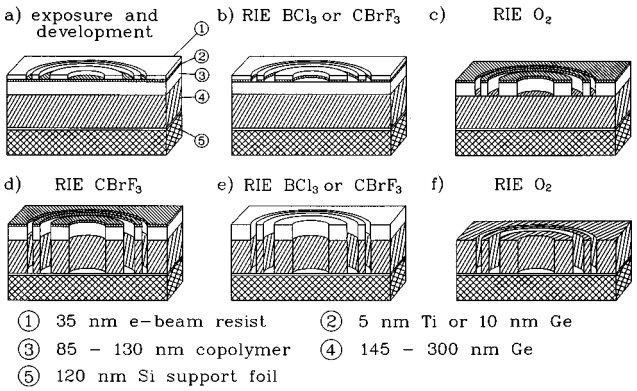

FIG. 7. Trilevel pattern transfer into germanium by RIE.

tures serve as a highly selective mask for the pattern transfer into Ge by RIE with $CBrF_3$ [Fig. 7(d)]. Figure 8 shows the Ge structures after removal of the remaining mask material [Figs. 7(e) and 7(f)].

V. DIFFRACTION EFFICIENCIES AND IMAGING PERFORMANCE

The first-order diffraction efficiencies of the ZPs were measured at 2.4 nm wavelength. Ni ZPs with outermost zone widths of 30 nm (zone height 130 nm) and 40 nm (zone height 150 nm) achieved diffraction efficiencies of 11% and 15%. In comparison with the model calculations shown in Fig. 1 we obtained 80%–90% of the theoretical efficiencies. The diffraction efficiencies of Ge ZPs with the smallest zone widths of 19, 30, and 40 nm are 4% (zone height 145 nm), 10% (zone height 200 nm), and 14% (zone height 230 nm), which are 52%, 77%, and 87% from the theoretical values plotted in Fig. 1. Both nanostructuring processes result in high diffraction efficiencies and are very reproducible. We also conclude that the pattern transfer process for structures less than 30 nm has to be improved especially for high aspect ratios.

These Ni and Ge phase ZPs have been used as objectives in the x-ray microscope at BESSY for imaging biological, medical, and colloidal specimens. The imaging qualities were investigated with a Siemens star. Therefore, the smallest structures of about 24 nm width have been resolved (Fig. 3). Cryo x-ray imaging has also been performed with these optics and has shown the potential of x-ray microscopy for life sciences.[12]

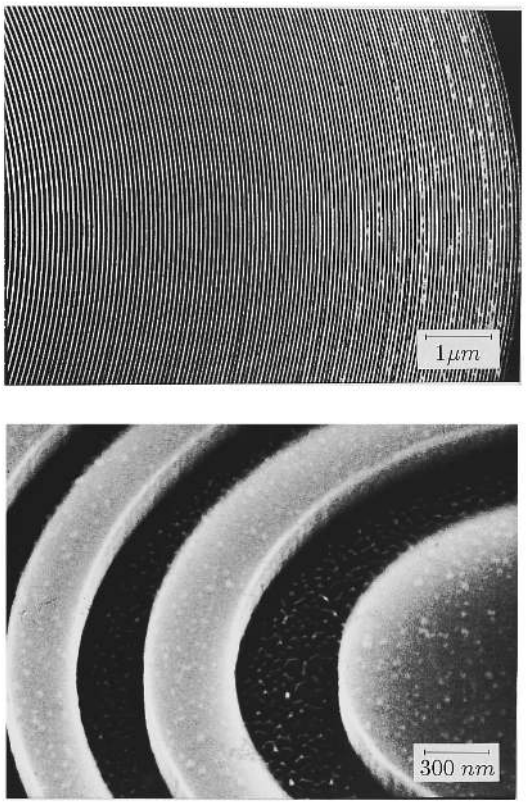

FIG. 8. SEM micrograph of the central and the outermost germanium zones after pattern transfer into a 220-nm-thick layer by RIE with $CBrF_3$.

ACKNOWLEDGMENTS

The authors thank G. Schmahl and D. Rudolph for their encouragement, and J. Herbst for assistance in performing the experiments. This work was funded by the German BMBF under Contract No. 05 5MGDXB 6.

[1] J. Maser, in *X-Ray Microscopy IV*, edited by V. V. Aristov and A. I. Erko (Chernogolovka, Moscow Region: Bogorodski Pechatnik, 1995).
[2] G. Schneider (unpublished).
[3] F. Emoto, K. Gamo, S. Namba, N. Samoto, R. Shimizu, and N. Tamura, Microelectron. Eng. **3**, 17 (1985).
[4] E. Roberts, Am. Chem. Soc. Org. Coat. Prepr. **33**, 359 (1973).
[5] W. M. Moreau, *Semiconductor Lithography* (Plenum, New York, 1988), pp. 132–134.
[6] C. David, J. Thieme, P. Guttmann, G. Schneider, D. Rudolph, and G. Schmahl, Optik **91**, 95 (1992).
[7] C. David, R. Medenwaldt, J. Thieme, P. Guttmann, D. Rudolph, and G. Schmahl, J. Opt. **23**, 255 (1992).
[8] C. David, B. Kaulich, R. Medenwaldt, M. Hettwer, N. Fay, M. Diehl, J. Thieme, and G. Schmahl, J. Vac. Sci. Technol. B **13**, 2762 (1995).
[9] E. Anderson and D. Kern, *X-Ray Microscopy III*, edited by A. G. Michette, G. R. Morrison, and C. J. Buckley (Springer, Berlin, 1992), pp. 313–315.
[10] D. M. Tennant, E. L. Raab, M. M. Becker, M. L. O'Malley, J. E. Bjorkholm, and R. W. Epworth, J. Vac. Sci. Technol. B **8**, 1970 (1990).
[11] J. Thieme *et al.*, in Ref. 1.
[12] G. Schneider, B. Niemann, P. Guttmann, D. Rudolph, and G. Schmahl, Synch. Radiat. News **8**, No. 3 (1995).